Supporting Information for

Carrier Transport in PbS and PbSe QD films Measured by Photoluminescence Quenching

Jing Zhang, Jason Tolentino, E. Ryan Smith, Jianbing Zhang, Matthew C. Beard, Arthur J. Nozik, Matt Law, Justin C. Johnson*

National Renewable Energy Laboratory, 15013 Denver West Pkwy, Golden CO 80401

Department of Chemistry and Biochemistry, University of Colorado, Boulder, CO 80301

Department of Chemistry, University of California, Irvine, CA 92697

School of Optical and Electronic Information, Huazhong University of Science and Technology, 1037 Luoyu Road, Wuhan, Hubei 430074, China

I. Discussion of Transport Mechanism

Since the value of ν (the exponent in the activated hopping equation) could not easily be determined from the global fits due to the large number of parameters, we used the approach described in Zhang et al.[1] and Liu et al.[2] The exponential term was isolated from equation 3 by taking $1/I_{PL}$ and subtracting $1/I_{PL}(T=0)$, which equals $\alpha/k_{rr}\ \exp(-T^*/T)^{\nu}$. This relationship resembles that of conductance *G* vs. temperature, and thus taking the derivative *d (Ln G) /d (Ln T)* and plotting on a double logarithmic scale produces a slope that is equal to *ν*. The scatter in the data points prohibits a determination of ν with uncertainty smaller than 0.25, which would be necessary to assign the transport regime. The values generally clustered between 0.4 and 1, which does not rule out NNH (ν = 1) or ES VRH (ν = 0.5). A value of ν = 0.67 is predicted in some situations.[3]

ES VRH was previously reported in dark conductance measurements on weakly coupled PbSe and CdSe QD films,[4-5] although a crossover to the Mott VRH (*ν* = 0.25) regime can sometimes be seen. Mott VRH should be active only above $T_c = {e^4 g_0 a}/{(4\pi\epsilon_0\epsilon)^2 k_B}$, where g_0 is the density of states (~3×10^{20} eV^{-1} cm^{-3}), ϵ is the dielectric constant (~11)[6] and *a* is the localization length (~ QD diameter).[2] There is some uncertainty in g_0 and ϵ, but T_c ~ 180 K is a lower limit, thus a change in the slope of ${\partial(\ln k_{CT})}/{\partial(lnT)}$ is unlikely to be seen since it would occur at temperature for which the PL is strongly quenched. A crossover to Arrhenius behavior could instead occur at $T_A = \left(\frac{a}{2d}\right) T^*$ ~ 100 K [5] but the exact crossover is difficult to quantify from PL data alone since it also likely occurs at a temperature where PL is strongly quenched.

II. Further Global Fitting Information

Fits of $\Phi_{PL}(T)$ data to equation 3 with α as a global variable produced reasonable agreement for short ligands but not for longer ligands (Figure S2). Thus, fits with E_a as a global variable (as in Figure 3 in the main text) were preferred.

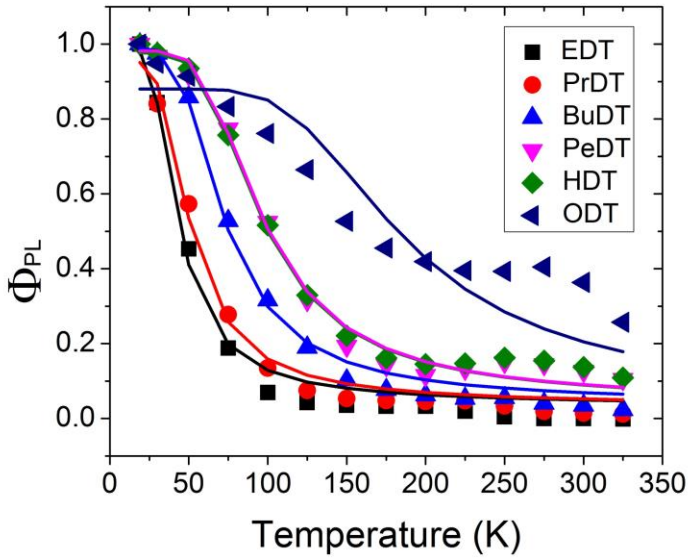

Figure S1. Simultaneous fit with E_a freely varying and α global for a set of 3.8 nm PbS QDs .

III. Temperature-dependent PL Quenching Data for Ligand-Exchanged PbSe QD films

As mentioned in the main text, PL quenching data for PbSe QD films was measured, but reliable Φ_{PL} values could not be obtained. Fits of $I_{PL}(T)$ with equation 3 were still performed and found to be satisfactory, but for determination of α, $\Phi_{PL}(T = 18\ K)$ was assumed to follow the same trend with ligand length as with PbS (Table 1). Using this approximation, the values for E_a, T^*, and β were obtained (Table S1). The maximum α was found to be roughly 10^{12} s^{-1} for all samples. The fit of β vs. d on a semilog plot produced approximately linear trends (Figure S2). As with the smallest PbS QD sample, the fits for the 2.0 nm PbSe QD sample were quite poor for longer ligands at temperatures below 100 K. Thus, only samples exchanged with ligands EDT, PrDT, and BuDT were included in the fit.

Table S1. Photophysical data and extracted fit parameters for 2.0 nm and 2.5 nm PbSe QD films. See main text for description of fits.

Peak abs /eV	$FWHM_{abs}$ /eV	$FWHM_{PL}$ /eV	E_D/ meV	E_C / meV	E_a/meV (v = 1)	k_{NR} (sec^{-1})	β / $Å^{-1}$
1.36	218	81	93	82	40	2.7×10^6	1.1±0.17
1.2	184	72	78	56	54	3.3×10^6	1.3±0.12

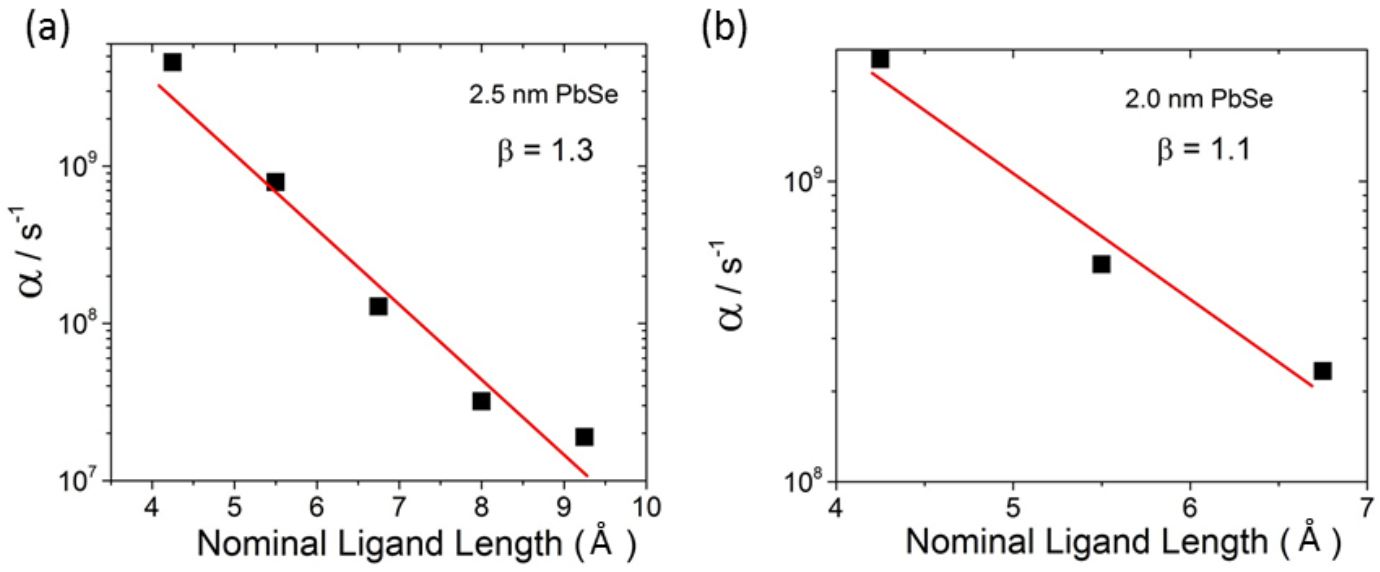

Figure S2. Results of fitting to equation 3 for PbSe QD films.

IV. PL Peak Shift and Quantum Yield Correlation

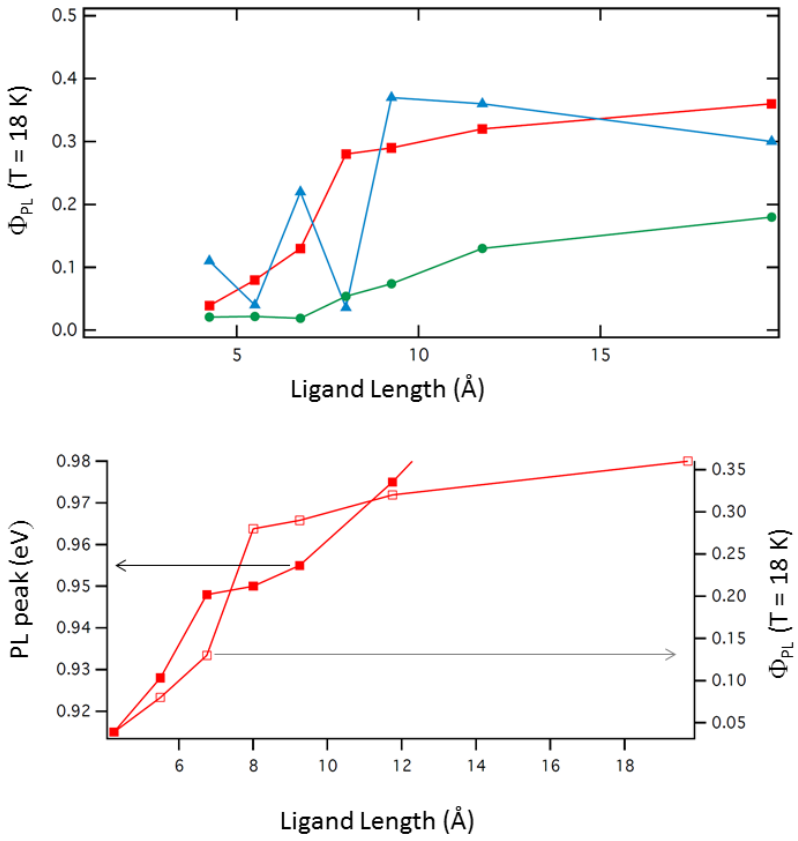

Figure S3. (a) Φ_{PL} values from Table 1 are plotted versus ligand length. (b) PL peak position vs. the ligand length (filled square) overlaid with Φ_{PL} data (open squares) which demonstrates a correlation between the interparticle coupling and emission probability.

V. FET Measurements

QD films were dip coated onto degenerately doped silicon substrates that were coated with a 200-nm-thick SiO_2 gate oxide and patterned with source/drain electrodes (3 nm Ti/40 nm Au; 5, 10, or 25 μm channel length, 1000 μm width). Unwanted areas of films were removed with a swab with 50 μL of dry hexane. FET measurements were performed at room temperature in a glovebox using a homemade 4-point probe station using a Keithley 2636A dual-channel SourceMeter driven by a custom made LabVIEW software. Consistent with previous results,[7-8] we found the source-drain currents of these FETs to be time dependent when changing the gate voltage. I_D-V_{SD} and I_D-V_G curves were acquired as quickly as possible with a scan rate of 50 Vs^{-1} to minimize effects of the transient processes. Electron and hole mobilities μ_{lin} were calculated from the transfer curves acquired at positive and negative V_{SD}, respectively, according to the gradual channel approximation equation in the linear regime,

$$\frac{\partial I_D}{\partial V_G}_{V_{SD}=constant} = \frac{W C_{OX} V_{SD}}{L} \mu_{lin}$$

where W is the channel width, L is the channel length, and C_{OX} is the capacitance per unit area of the gate oxide. The carrier mobilities reported here are measured with a channel length, L, of 5 μm and averaged between 5 devices for each ligand treatment.

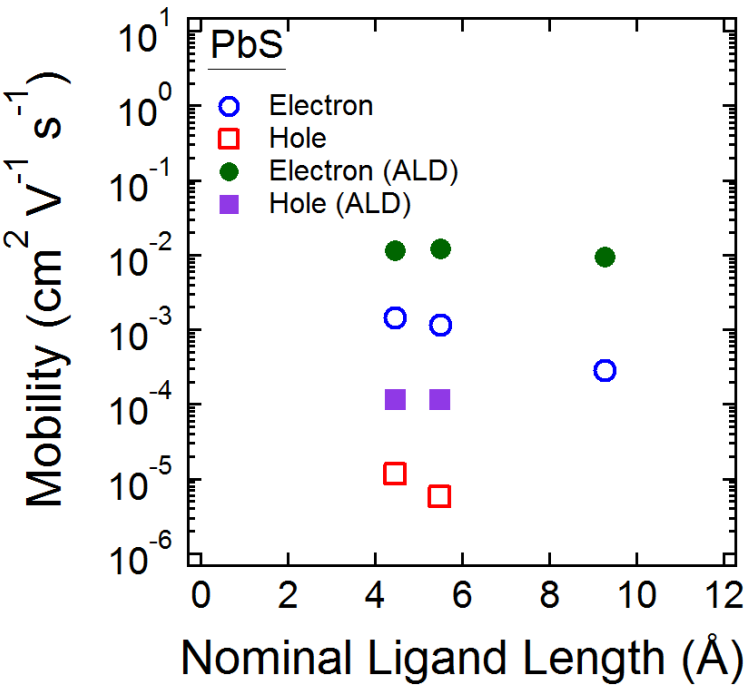

Figure S4. FET data for alkanedithiol-treated (open circles) and alkanedithiol/ALD treated (filled shapes) 3.8 nm PbS QD film samples at room temperature.

References

1. Zhang, X.; Manno, M.; Baruth, A.; Johnson, M.; Aydil, E. S.; Leighton, C. Crossover from Nanoscopic Intergranular Hopping to Conventional Charge Transport in Pyrite Thin Films. *ACS Nano.* **2013,** *7*, 2781-2789.
2. Liu, H.; Pourret, A.; Guyot-Sionnest, P. Mott and Efros-Shklovskii Variable Range Hopping in Cdse Quantum Dots Films. *ACS Nano.* **2010,** *4*, 5211-5216.
3. Houtepen, A. J.; Kockmann, D.; Vanmaekelbergh, D. Reappraisal of Variable-Range Hopping in Quantum-Dot Solids. *Nano Lett.* **2008,** *8*, 3516-3520.
4. Kang, M. S.; Sahu, A.; Norris, D. J.; Frisbie, C. D. Size- and Temperature-Dependent Charge Transport in Pbse Nanocrystal Thin Films. *Nano Lett.* **2011,** *11*, 3887-3892.
5. Yu, D.; Wang, C. J.; Wehrenberg, B. L.; Guyot-Sionnest, P. Variable Range Hopping Conduction in Semiconductor Nanocrystal Solids. *Phys. Rev. Lett.* **2004,** *92*.
6. Luther, J. M.; Law, M.; Beard, M. C.; Song, Q.; Reese, M. O.; Ellingson, R. J.; Nozik, A. J. Schottky Solar Cells Based on Colloidal Nanocrystal Films. *Nano Lett.* **2008,** *8*, 3488-3492.

7. Osedach, T. P.; Zhao, N.; Andrew, T. L.; Brown, P. R.; Wanger, D. D.; Strasfeld, D. B.; Chang, L. Y.; Bawendi, M. G.; Bulovic, V. Bias-Stress Effect in 1,2-Ethanedithiol-Treated Pbs Quantum Dot Field-Effect Transistors. *ACS Nano.* **2012,** *6,* 3121-3127.
8. Law, M.; Luther, J. M.; Song, O.; Hughes, B. K.; Perkins, C. L.; Nozik, A. J. Structural, Optical, and Electrical Properties of Pbse Nanocrystal Solids Treated Thermally or with Simple Amines. *J. Am. Chem. Soc.* **2008,** *130,* 5974-5985.